Entrainment in a Chemical Oscillator Chain with a Pacemaker

Hirokazu Fukuda,*,† Naoki Tamari,† Hiroki Morimura,† and Shoichi Kai†,‡,§

Department of Applied Quantum Physics and Nuclear Engineering, Faculty of Engineering, and Department of Life Engineering, Graduate School of Systems Life Sciences, Kyushu University, Fukuoka 812-8581, Japan

Received: May 24, 2005; In Final Form: September 26, 2005

Entrainment by a pacemaker was investigated experimentally and numerically in a chain of chemical oscillators using coupled discrete Belousov−Zhabotinsky reaction oscillators. The spontaneous frequency of each oscillator depended on the concentration of catalyst ions. The coupling strengths among the nearest neighbor oscillators were controlled by changing the spacing distance (*d*) between beads. When the coupling strength was sufficiently strong, the pacemaker entrained other oscillators in the chain. Subsequently, the trigger waves propagating from a pacemaker were observed. The range of trigger wave propagation area, i.e., the number of entrained oscillators, depended on *d*. Numerical simulation for the system described the experimental results well. Furthermore, photic noise maximized the strength of entrainment at an optimal noise intensity.

Introduction

Pacemakers, oscillators with higher frequency than others, entrain and coordinate oscillators in coupled oscillator systems.[1,2] Especially in biological systems, it is well-known that the pacemaker (master oscillator) often plays various important roles.[3,4] Recently, the functions of pacemakers in neural networks with complex topology have been investigated using a phase oscillator model.[2] They were found to possess a critical coupling strength for entrainment of the entire system.

Belousov−Zhabotinsky (BZ) reaction systems are also well-known systems for the study of nonlinear dynamics, e.g., entrainment of many chemical oscillators.[5−7] To mimic the above biological aspects, BZ systems are frequently used.[8] A target pattern in the BZ medium is the typical spatiotemporal structure coordinated by a pacemaker in coupled chemical oscillators.[9] The pacemaker at the core in the target pattern is a source of the propagating trigger waves; such dynamics of spatially continuous BZ systems have become well understood. The discrete BZ oscillator system, however, remains enigmatic; recently, it has been studied using cation-exchange beads.[10−18] In such a bead-oscillators system, trigger wave propagation has been observed to arise from successive entrainment of oscillators.[14] The maximum area of the propagation of the trigger waves in the two-dimensional lattice of bead oscillators has been described as a function of the coupling strength.[18] The bead-oscillators systems might then have additional degrees of freedom because they include the finite size of the bead, characteristic scales of the reaction-diffusion field, and the resulting pattern fields and the system size. All of those factors might then engender various spatiotemporal structures.[19,20] Therefore, the bead-oscillators systems might show rich dynamic features that are indescribable in the context of the simple phase oscillator model. In addition, optimal noise application reportedly enhances entrainment in coupled bead-oscillators,[16−18] the so-called stochastic synchronization.[21−27] Nevertheless, such interesting dynamics related to multiple characteristic scales, as well as noise, have not been investigated well.

In the present study, we experimentally and numerically examine entrainment dynamics in 1D coupled-discrete BZ chemical oscillators that are distributed spatially in a chain with spacing *d* to clarify the roles of a pacemaker and its dynamics. Coupling between two oscillators via mass diffusion of chemicals can be realized and varied by *d* in this case.

Experimental Section

Chemicals and their concentrations were prepared as 0.83 M H_2SO_4, 0.28 M $KBrO_3$, 0.06 M KBr, and 0.11 M $CH_2(COOH)_2$ at room temperature of 24 ± 1 °C. To absorb the catalyst into cation-exchange beads (50 W×4; Muromachi Technos Co. Ltd.), beads with diameter *a* (0.90 ± 0.01 mm) were immersed for more than 6 h with stirring in a ruthenium(II)−bipyridyl complex ($Ru(bpy)_3^{2+}$) solution controlled to the desired concentration. To obtain a regular and precious arrangement of beads in the BZ solution, we prepared glass boards (40 mm × 40 mm × 5 mm) with regularly arranged holes (diameter 0.60 ± 0.01 mm) using microblasting technology. A bead was placed in each hole on the board, which was then immersed into the BZ solution (20 mL) in a Petri dish (diameter 5.8 cm) on the level desk; the layer thickness of BZ solution covering the glass board was about 5.6 mm. We paid careful attention to suppress hydrodynamic instabilities in the BZ solutions as long as we could. Figure 1 shows a chain of coupled bead-oscillators with a pacemaker. The oscillator 0 is the pacemaker, and oscillators 1−10 are the slaved oscillators. They were coupled to the nearest neighbor beads via mass diffusion of chemicals with spacing *d*. The spontaneous frequency of each bead depends on the concentration of the catalyst ions: the lower the concentration in the bead, the higher the frequency of its oscillation. The pacemaker bead therefore usually has a concentration of catalyst lower than that in the slaved beads. The natural period of the pacemaker with 1.73×10^{-5} mol/g of $Ru(bpy)_3^{2+}$ was 210 ± 10 s, whereas that of the slaved oscillator with 2.3×10^{-5} mol/g of $Ru(bpy)_3^{2+}$ 256 ± 13 s.

Oscillation was recorded using a CCD camera, the images of which were stored for later analysis on a videotape and a

* To whom correspondence should be addressed. Present address: Graduate School of Life and Environment Sciences, Osaka Prefecture University, Sakai 599-8531, Japan. Email: fukuda@bioinfo.osakafu-u.ac.jp.
† Faculty of Engineering.
‡ Graduate School of Systems Life Sciences.
§ Email: kaitap@mbox.nc.kyushu-u.ac.jp.

10.1021/jp052717k CCC: $30.25
Published on Web 11/15/2005

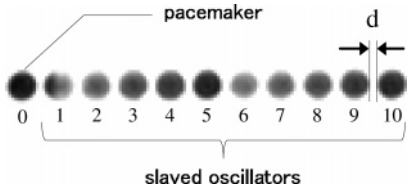

Figure 1. Chain of Belousov−Zhabotinsky bead-oscillators with a pacemaker (master oscillator). The oscillator 0 is the pacemaker and oscillators 1−10 are the slaved oscillators. The natural periods of the pacemaker and the slaved oscillator are about 210 and 256 s, respectively. The darker area demarcates the oxidation state; the lighter area is the reduction state.

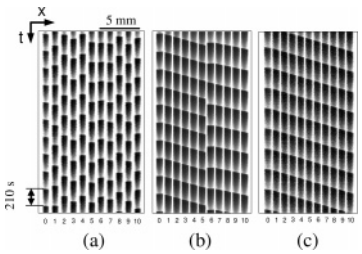

Figure 2. Spatiotemporal plots of oscillations in a chain of coupled bead-oscillators with a pacemaker (no. 0). In (a), (b), and (c), the spacing distances d are 0.2, 0.06, and 0.04 mm, respectively. The darker area demarcates the oxidation state; the lighter area is the reduction state.

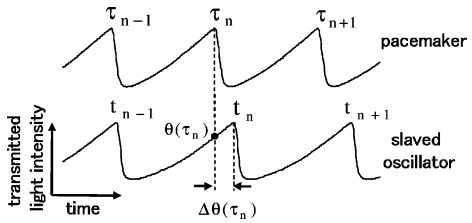

Figure 3. Definition of the relative phase $\theta(\tau_n)$ and the phase difference $\Delta\theta(\tau_n)$.

computer hard disk. The time sequence of optical intensity from each oscillator was obtained by averaging the gray level of the 8×8 pixels at the central region on the bead surface. To avoid the transient process, the analyses for respective oscillators were performed after waiting for a sufficiently long period; the time duration was 10 000−20 000 s from initiation.

Results and Discussion

Figure 2 shows typical examples of the spatiotemporal plots of oscillations in a chain of bead-oscillators with a pacemaker. In the large spacing of $d = 0.2$ mm, the coupling strength was too weak to entrain slaved oscillators using a pacemaker. For that reason, all beads oscillated in their own frequencies (Figure 2a). As d decreases, the pacemaker oscillator entrained more of the slaved oscillators from the left side in succession. At $d = 0.06$ mm, the pacemaker oscillator entrained five slaved oscillators (oscillators 1−5). Subsequently, the trigger waves began propagating from the pacemaker (Figure 2b). We have two different domains in this case. In $d = 0.04$ mm, all oscillators were entrained by the pacemaker and the trigger waves traveled all over the beads (Figure 2c). Therefore, we have a single domain in this case. The velocity of propagating trigger waves was about 4×10^{-2} mm/s.

To characterize entrainment by a pacemaker, we define the relative phase $\theta(\tau_n)$ of the slaved oscillator for the standard time based on the pacemaker, as shown in Figure 3. Here τ_n is the time of the nth oscillation of the pacemaker, and t_n represents that of the slaved oscillator. The phase difference between the

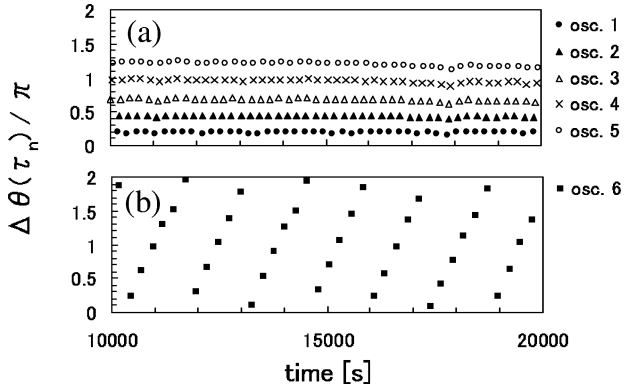

Figure 4. Time series of the phase difference $\Delta\theta(\tau_n)$ between the pacemaker and the slaved oscillator with $d = 0.06$ mm. Points (a) and (b) show, respectively, $\Delta\theta(\tau_n)$ values for oscillators 1−5 and the oscillator 6.

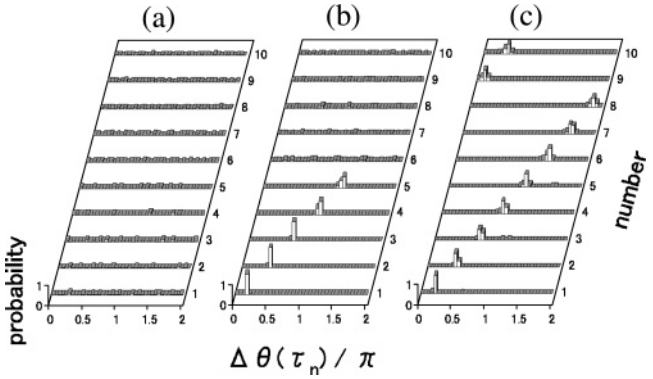

Figure 5. Probability of $\Delta\theta(\tau_n)$ for each slaved oscillator. In (a), (b), and (c), the respective spacing distances d are 0.2, 0.06, and 0.04 mm.

pacemaker and the slaved oscillator is then determined as $\Delta\theta(\tau_n)$ in Figure 3.

Figure 4 shows the time series of $\Delta\theta(\tau_n)$ for the slaved oscillators 1−6 in Figure 2b. The oscillators 1−5 show no temporal development of $\Delta\theta(\tau_n)$ (Figure 4a), verifying that these were perfectly entrained by the pacemaker. The systematic and constant phase difference between oscillators is observable. In contrast, oscillator 6 shows a continuous shift of $\Delta\theta(\tau_n)$, as shown in Figure 4b. That is, oscillator 6 was not entrained at all by the pacemaker.

Figure 5 shows the probability of $\Delta\theta(\tau_n)$ for each slaved oscillator. In $d = 0.2$ mm, because of the lack of entrainment, no peak existed in the probability for each slaved oscillator, as shown in Figure 5a. In $d = 0.06$ mm, peaks were observed in oscillators 1−5; no peak was observed in oscillators 6−10 (Figure 5b). In $d = 0.04$ mm, peaks were observed in all slaved oscillators, indicating that all slaved oscillators were entrained by the pacemaker.

Next, we introduce the time-averaged entrainment rate r defined as

$$re^{i\Delta\Psi} = \langle e^{i\Delta\theta(\tau_n)} \rangle \tag{1}$$

where $\Delta\Psi$ is the phase difference at the peak of probability of $\Delta\theta(\tau_n)$ and the bracket denotes the average over time. For $r \geq 0.8$, we assume that the slaved oscillator is sufficiently entrained by the pacemaker and count the number of entrained oscillators as N_E. Figure 6 shows r for each slaved oscillator with various spacings d. At $d = 0.2$ mm (Figure 6a), r and the number of the slaved oscillators entrained by a pacemaker, N_E, are 0. At $d = 0.06$ mm, shown in Figure 6b, N_E is 5, indicating that the

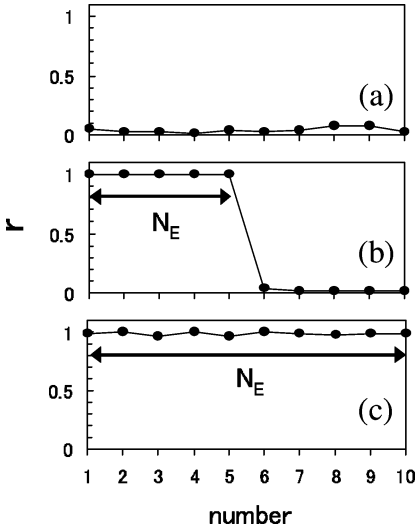

Figure 6. Entrainment rate r of the slaved oscillators. In (a), (b), and (c), the respective spacing distances d are 0.2, 0.06, and 0.04 mm. N_E is the number of the slaved oscillators entrained by a pacemaker.

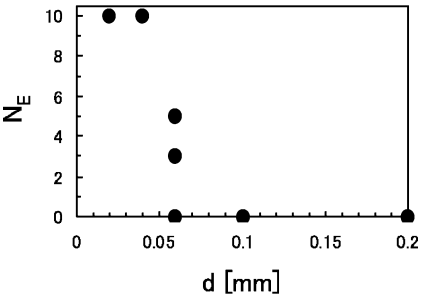

Figure 7. N_E as a function of d in the chain of bead-oscillators with a pacemaker.

slaved oscillators 1−5 were entrained by the pacemaker. At $d = 0.04$ mm (Figure 6c), N_E is 10, indicating that all slaved oscillators were entrained by the pacemaker. Figure 7 shows N_E as a function of d. The value of N_E decreases suddenly at $d = 0.06$ mm with increasing d. Therefore, the critical spacing $d_c \approx 0.06$ mm. The large fluctuation of N_E was observed only near d_c; that is, N_E showed a great change for each trial, indicating that N_E near the critical spacing d_c becomes extremely sensitive to the experimental conditions. This experimental observation will be elucidated in the next section.

Numerical Simulation

Model. In the photosensitive BZ reaction using $Ru(bpy)_3^{2+}$ as a catalyst, constant light illumination suppresses oxidation through photochemical production of Br^-, an inhibitor of autocatalysis in the BZ reaction. We conducted numerical simulation using a modified dimensionless photosensitive Oregonator model to investigate entrainment in a BZ oscillators chain with a pacemaker:[28,29]

$$\epsilon \dot{x}_i = x_i(1 - z_i/c_i) - x_i^2 + y_i(q - x_i) + p_2\phi + \epsilon \frac{D}{d^2} \sum_{<j>} (x_j - x_i) \quad (2)$$

$$\epsilon' \dot{y}_i = 2hz_i - y_i(q + x_i) + p_1\phi + \epsilon' \frac{D}{d^2} \sum_{<j>} (y_j - y_i) \quad (3)$$

$$\dot{z}_i = x_i(1 - z_i/c_i) - z_i + (p_1/2 + p_2)\phi \quad (4)$$

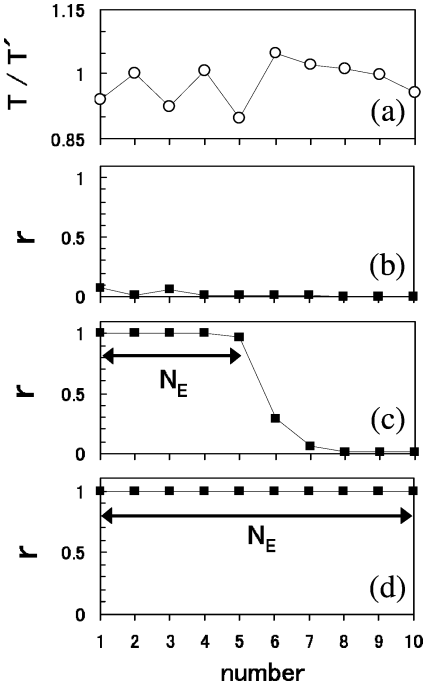

Figure 8. Entrainment rate r of slaved oscillators obtained from numerical calculation. (a) Spontaneous period T of each slaved oscillator given by a random choice of $\{c_i\}$, where $T' = 51.61$ indicates the period of the oscillator with $c_i = 0.5$. In (b), (c), and (d), the values of d were 30, 12, and 10, respectively. The pacemaker (no. 0) had the concentration of the catalyst $c_0 = 0.14$ and the spontaneous period $T_0 = 41$.

Therein, x_i, y_i, and z_i represent, respectively, the concentrations of the activator, the inhibitor, and the oxidized catalyst of the oscillator i; ϵ and ϵ' are scaling constants ($\epsilon = 4.29 \times 10^{-1}$, $\epsilon' = 2.32 \times 10^{-3}$); q is another scaling constant ($q = 9.52 \times 10^{-5}$); h is a stoichiometric factor ($h = 0.5$); and p_1 and p_2 ($p_1 = 1.12 \times 10^{-1}$, $p_2 = 6.89 \times 10^{-1}$) represent, respectively, the coefficients of photosensitivity determined by the combination of concentrations among bromate, sulfuric acid, and bromomalonic acid; ϕ is the light flux. The total catalyst ion concentration of the oscillator i is c_i, which determines the spontaneous period of the oscillator i. Depending on c_i, the pacemaker and slaved oscillators were determined. The catalyst ions are absorbed in the beads and coupling between oscillators is mediated by respective diffusions of x and y. For simplification of the calculation, we assumed each bead as a point oscillator and the coupling strength is given as D/d^2, where D and d are the effective diffusion constants including geometric contributions as well and the spacing between oscillators respectively.[18] In our calculation, here $D = 1$. $\Sigma_{<j>}$ indicates the summation over the nearest-neighbors j of the oscillator i.

Computer simulation was performed using the fourth-order Runge−Kutta method with the time step $\Delta t = 0.005$. Statistical quantities were calculated from a run of 5.8×10^6 time steps after discarding the initial 2×10^5 time steps as a transient.

Entrainment in a Chain of Chemical Oscillators with a Pacemaker. Simulation has been done with changing the spacing d to check the aspect in Figure 6. We performed simulation in an oscillator chain consisting of a pacemaker and 10 slaved oscillators. Figure 8a shows spontaneous periods of the slaved oscillators with a random and arbitrary choice of the concentration $\{c_i\}$ of the catalyst in a chain. The fluctuation in period (about 5% of average) is well-reproduced in the experimental condition. Here, the distribution of $\{c_i\}$ is given as a Gaussian distribution with an average of 0.5 and a standard deviation of 0.1. Figure 8b−d shows the entrainment rate r as

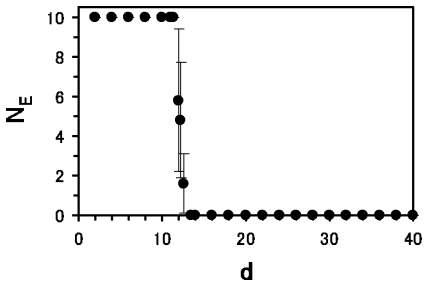

Figure 9. N_E as a function of d in the chain of chemical oscillators with a pacemaker obtained from numerical calculation. Error bars show the standard deviations of N_E with a set of five different $\{c_i\}$ at each spacing d.

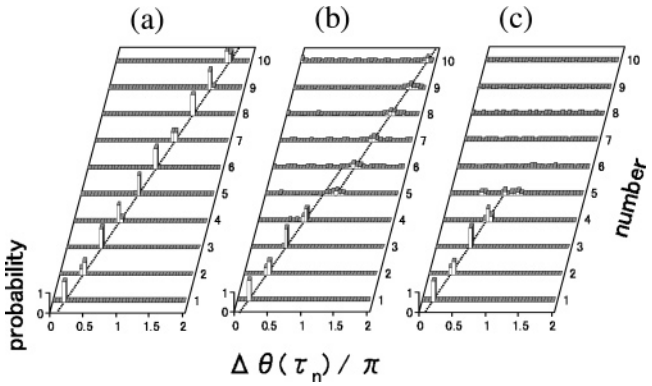

Figure 10. Probability of $\Delta\theta(\tau_n)$ for each slaved oscillator obtained from numerical calculation. In (a), (b), and (c), α are 0, 0.9 and 1.5, respectively. The other parameter values are $\phi_0 = 1.668 \times 10^{-3}$, $c_0 = 0.14$, $c_1 = ... = c_{10} = 0.5$, $d = 9.5$ and $\beta = 0$.

a function of d. In large spacing ($d = 30$), no entrainment by the pacemaker exists (Figure 8b). As d decreases, the pacemaker entrains the slaved oscillators and N_E increases. At critical spacing, $d = 12$, the slaved oscillators 1−5 were entrained by the pacemaker (Figure 8c). In that case, the entrainment stopped at the oscillator 6 because the large difference of their own periods between the oscillators 5 and 6 occurred accidentally. Figure 9 shows N_E as a function of d. At $d = 12$, the value of N_E decreased suddenly and the large fluctuation of N_E was observed. Because of fluctuations of spontaneous periods, N_E varies at the critical spacing. Therefore, N_E at the critical spacing d_c is strongly sensitive to the distribution of the spontaneous periods, which well describes the experimental observation in Figure 7.

Noise-Induced Entrainment in a Chain of Chemical Oscillators with a Pacemaker. To investigate the noise effect for entrainment by the pacemaker, the random noise of light illumination was applied as follows:

$$\phi = \phi_0(\alpha + \beta\xi(\delta)) \tag{5}$$

where ϕ_0 and α are constant values, both of which define a Hopf bifurcation point of the system. Here, β is the amplitude of noise $\xi(\delta)$, which is the random value equally distributed among −1 and 1; δ is the interval of random steps ($\delta = 1$). When α increases, the period of oscillations increases gradually and then the oscillations suddenly cease at $\alpha = 1$.

Figure 10 shows the probability of $\Delta\theta(\tau_n)$ for each slaved oscillator. We inferred that all slaved oscillators had equal catalyst concentration to simplify simulation. In the absence of the light illumination ($\alpha = 0$, $\beta = 0$), all slaved oscillators showed the peak of $\Delta\theta(\tau_n)$, which shifted continuously as the number of oscillators increased (Figure 10a). All slaved oscillators were entrained by the pacemaker and the trigger waves propagated from the pacemaker to the terminal oscillator 10. When constant light illumination was applied only at oscillator 5 ($\alpha = 0.9$, $\beta = 0$), entrainment of oscillator 5 was suppressed, as shown in Figure 10b. The phase jump was then observed between the oscillators 5 and 6, indicating discontinuity of the trigger wave propagation. At the strong intensity of the light ($\alpha = 1.5$, $\beta = 0$), however, trigger waves from the pacemaker were not interpreted between them (Figure 10c).

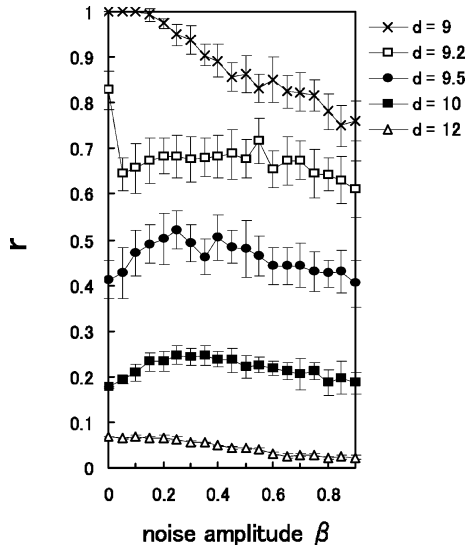

Figure 11. Entrainment rate r of the oscillator 10 as a function of noise amplitude β. The noisy light illumination was applied only in oscillator 5. Error bars show the standard deviations of r with a set of 3−25 random numbers at each noise amplitude. The parameter values are $\alpha = 0.99$, $\phi_0 = 1.668 \times 10^{-3}$, $c_0 = 0.14$ and $c_1 = ... = c_{10} = 0.5$.

Figure 11 shows the entrainment rate r of the terminal oscillator 10 for five different spacings d as a function of the noise amplitude β. For $d = 9.5$ and 10, maxima r are observable as a function of β; an optimal noise amplitude exists. For other spacings, no optimal noise amplitude exists. Results indicate that an optimal spacing (i.e., optimal coupling strength) does exist for enhancing noise-induced entrainment. We call "noise-induced entrainment" for any value of r when r in the presence of externally applied noises is larger than the expected value of r in the absence of noises. Similar aspects have been reported experimentally in 10 × 10 lattice oscillator systems.[18]

Conclusions

We studied entrainment phenomena in a chain of chemical bead-oscillators, one of which was set as a pacemaker. The pacemaker entrained all oscillators when the distance d between the beads was sufficiently small and the trigger waves propagated periodically from the pacemaker to the terminal oscillator. No entrainment occurred in the whole chain of BZ oscillators beyond the critical spacing d_c. Large fluctuation of entrainment was observed near d_c. In the numerical simulations using the modified photosensitive Oregonator model, the constant light illumination suppressed the entrainment. However if noisy illumination was superimposed on the constant light, entrainment by the pacemaker was maximized at an optimal noise amplitude. That is, stochastic synchronization was observed.

Acknowledgment. We are grateful to Prof. T. Amemiya at Yokohama National University for his valuable suggestions and comments about the model. This work was supported in part

by a Research Fellowship of the Japan Society for the Promotion of Science for Young Scientists (no. 0307712).

References and Notes

(1) Pikovsky, A.; Rosenblum, M.; Kurths, J. *Synchronization: A Universal Concept in Nonlinear Science*; Cambrige University Press: Cambridge, 2001.

(2) Kori, H.; Mikhailov, A. S. *Phys. Rev. Lett.* **2004**, *93*, 254101.

(3) Winfree, A. T. *The Geometry of Biological Time*; Springer: New York, 1980.

(4) Aoyagi, T.; Takekawa, T.; Fukai, T. *Neural Comput.* **2003**, *15*, 1035.

(5) Sagués, F.; Epstein, I. R. *Dalton Trans.* **2003**, 1201.

(6) Kiss, I. Z.; Zhai, Y.; Hudson J. L. *Science* **2002**, *296*, 1676.

(7) Zhai, Y.; Kiss, I. Z.; Daido, H.; Hudson J. L. *Physica D* **2005**, *205*, 57.

(8) Suzuki, N.; Hirata, M.; Kondo, S. *Proc. Natl. Acad. Sci. U.S.A.* **2003**, *100*, 9680.

(9) Zaikin, A. N.; Zhabotinsky, A. M. *Nature (London)* **1970**, *225*, 535.

(10) Stuchl, I.; Marek, M. *J. Chem. Phys.* **1982**, *77*, 2956.

(11) Yoshimoto, M.; Yoshikawa, K.; Mori, Y.; Hanazaki, I. *Chem. Phys. Lett.* **1992**, *189*, 18.

(12) Yoshimoto, M.; Yoshikawa, K.; Mori, Y. *Phys. Rev. E* **1993**, *47*, 864.

(13) Maselko, J.; Reckley, J. S.; Showalter, K. *J. Phys. Chem.* **1989**, *93*, 2774.

(14) Nishiyama, N.; Matsuyama, T. *J. Chem. Phys.* **1997**, *106*, 3427.

(15) Miyakawa, K.; Okabe, T.; Mizoguchi, M.; Sakamoto, F. *J. Chem. Phys.* **1995**, *103*, 9621.

(16) Fujii, K.; Hayashi, D.; Inomoto, O.; Kai, S. *Forma* **2000**, *15*, 219.

(17) Fukuda, H.; Nagano, H.; Kai, S. *J. Phys. Soc. Jpn.* **2003**, *72*, 487.

(18) Fukuda, H.; Morimura, H.; Kai, S. *Physica D* **2005**, *205*, 80.

(19) Maselko, J.; Showalter, K. *Nature* **1989**, *399*, 609.

(20) Aihara, R.; Yoshikawa, K. J. *Phys. Chem. A* **2001**, *105*, 8445.

(21) Neiman, A.; Silchenko, A.; Anishchenko, V.; Schimansky-Geier, L. *Phys. Rev. E* **1998**, *58*, 7118.

(22) Sakaguchi, H. *Phys. Rev. E* **2002**, *66*, 056129.

(23) Teramae, J.; Tanaka, D. *Phys. Rev. Lett.* **2004**, *93*, 204103.

(24) Kádár, S.; Wang, J.; Showalter, K. *Nature* **1998**, *391*, 770.

(25) Alonso, S.; Sendiña-Nadal, I.; Pérez-Muñuzuri, V.; Sancho, J. M.; Sagués, F. *Phys. Rev. Lett.* **2001**, *87*, 078302.

(26) Zhou, L. Q.; Jia, X.; Ouyang, Q. *Phys. Rev. Lett.* **2002**, *88*, 138301.

(27) Miyakawa, K.; Isikawa, H. *Phys. Rev. E* **2002**, *65*, 056206.

(28) Amemiya, T.; Ohmori, T.; Yamamoto, T.; Yamaguchi, T. J. *Phys. Chem. A* **1999**, *103*, 3451.

(29) Kawczyński, A. L.; Comstock, W. S.; Field, R. J. *Physica D* **1992**, *54*, 220.